



Published in final edited form as:

Neurobiol Sleep Circadian Rhythms. 2016 July 1; 1: .

EEG slow waves in traumatic brain injury: Convergent findings in mouse and man

Mo Modarres, PhD¹, Nicholas N. Kuzma, PhD^{2,3}, Tracy Kretzmer, PhD⁴, Allan I. Pack, MBChB PhD⁵, and Miranda M. Lim, MD, PhD^{2,6,7,*}

¹Brain Rehabilitation Research Center, North Florida/South Georgia Veterans Affairs Medical Center, Gainesville, FL

²Research Service, Veterans Affairs Portland Health Care System, Portland OR

³Department of Physics, Portland State University, Portland, OR

⁴Department of Mental Health and Behavioral Sciences, James A. Haley Veterans' Hospital, Tampa, FL

⁵Center for Sleep and Circadian Neurobiology, University of Pennsylvania, Philadelphia, PA

⁶Sleep Disorders Clinic, Division of Hospital and Specialty Medicine, Veterans Affairs Portland Health Care System, Portland OR

⁷Departments of Medicine, Neurology and Behavioral Neuroscience, and Oregon Institute of Occupational Health Sciences, Oregon Health & Science University, Portland, OR

Abstract

Objective—Evidence from previous studies suggests that greater sleep pressure, in the form of EEG-based slow waves, accumulates in specific brain regions that are more active during prior waking experience. We sought to quantify the number and coherence of EEG slow waves in subjects with mild traumatic brain injury (mTBI).

Methods—We developed a method to automatically detect individual slow waves in each EEG channel, and validated this method using simulated EEG data. We then used this method to quantify EEG-based slow waves during sleep and wake states in both mouse and human subjects with mTBI. A modified coherence index that accounts for information from multiple channels was calculated as a measure of slow wave synchrony.

Results—Brain-injured mice showed significantly higher theta:alpha amplitude ratios and significantly more slow waves during spontaneous wakefulness and during prolonged sleep deprivation, compared to sham-injured control mice. Human subjects with mTBI showed significantly higher theta:beta amplitude ratios and significantly more EEG slow waves while

*Corresponding author at: 3710 SW US Veterans Hospital Road, Mailcode P3-RD42, Portland, OR 97239, Tel.: +503 220 8262x57404. lmir@ohsu.edu.

Publisher's Disclaimer: This is a PDF file of an unedited manuscript that has been accepted for publication. As a service to our customers we are providing this early version of the manuscript. The manuscript will undergo copyediting, typesetting, and review of the resulting proof before it is published in its final citable form. Please note that during the production process errors may be discovered which could affect the content, and all legal disclaimers that apply to the journal pertain.

awake compared to age-matched control subjects. We then quantified the global coherence index of slow waves across several EEG channels in human subjects. Individuals with mTBI showed significantly less EEG global coherence compared to control subjects while awake, but not during sleep. EEG global coherence was significantly correlated with severity of post-concussive symptoms (as assessed by the Neurobehavioral Symptom Inventory scale).

Conclusion and implications—Taken together, our data from both mouse and human studies suggest that EEG slow wave quantity and the global coherence index of slow waves may represent a sensitive marker for the diagnosis and prognosis of mTBI and post-concussive symptoms.

Keywords

Traumatic brain injury; sleep; EEG; slow waves; coherence; translational

1. Introduction

Traumatic brain injury (TBI) is a worldwide problem and a major cause of disability among affected individuals. Mild, moderate or severe TBI often results in persistent sleep disturbances, which can significantly contribute to cognitive impairment, disability, and delay functional recovery¹⁻⁴. An estimated 42 million people worldwide suffer a mild TBI (mTBI) each year, and many of these go on to experience significant sleep-wake disturbances^{5,6}. However, the exact nature and mechanisms underlying sleep-wake disturbances in TBI are still unclear, and only recently have been the subject of descriptive and experimental studies⁷⁻¹¹. Furthermore, in mTBI, the clinical assessment currently lacks objective markers to confirm the diagnosis and aid in the prognosis of those who go on to develop persistent post-concussive symptoms.

A well-established mouse model of mTBI, lateral fluid percussion injury (FPI), exhibits similar pathology and behavioral deficits to those reported after human TBI^{12,13}. Our previous work established persistent changes in the sleep-wake cycle in mice following FPI, including, most notably, greater time spent in non-rapid eye movement (NREM) sleep and the inability to maintain continuous bouts of wakefulness⁷. Human studies also report increased sleep times following TBI, which may reflect increased sleep pressure^{14,15}. Regional slow waves have been implicated in sleep pressure, particularly during wakefulness^{16,17}. Here, we propose a new method utilizing quantitative analysis of the sleep-wake EEG, focusing on slow waves associated with chronic mTBI.

Previous studies applying quantitative EEG (QEEG) to TBI have primarily examined spectral power or frequency changes during sleep, for example noting enhanced beta power during non-rapid eye movement (NREM) sleep¹⁸. Several studies have indicated somewhat conflicting findings of less delta power during NREM sleep^{19,20} versus increased delta power during NREM sleep^{15,21}, with significant variability among subjects with mTBI, likely reflecting heterogeneity of the disease²². QEEG during the awake state in subjects with mTBI have shown attenuated posterior alpha or focal irregular slow wave activity or theta activity over the temporal region, increased delta power, and reduced alpha power²³⁻²⁶. Our method represents a novel approach from earlier QEEG methods in several ways: 1) we specifically counted the number of slow waves across a high-resolution time domain, instead

of averaging amplitudes over a large time scale, 2) our method calculates of a ‘global coherence measure’ of slow waves across multiple channels, as opposed to traditional coherence metrics which compare only pairs of channels, and 3) we compared QEEG of slow wave counts across both sleep and waking states, which to our knowledge, has not been done before in TBI.

In order to quantify slow waves and global slow wave coherence in sleep and wakefulness after TBI, we first examined EEG power spectral analyses comparing amplitude ratios across frequency bands in both mouse and human subjects after mTBI. Next, we designed and validated a method to quantify EEG slow waves. We then quantified slow waves in the sleep-wake EEG from both mouse and human subjects with mTBI. Finally, we designed a method to quantify the coherence of slow waves across multiple EEG channels in human subjects, and correlated this global coherence index with TBI symptom severity in individual subjects. The current experiments were designed to assess the utility of EEG slow wave counts and coherence during sleep and wakefulness in the diagnosis and prognosis of mTBI.

2. Materials and methods

2.1. Animals

Animal experiments were performed on 10 week old, 25 g, male C57BL/J6 mice (Jackson Laboratory). The animals were housed in a room that was maintained at an ambient temperature of $23 \pm 1^\circ\text{C}$ with a relative humidity of $25 \pm 5\%$ and that was on an automatically controlled 12-h light/12-h dark cycle (lights on at 07:00 hours, illumination intensity ≈ 100 lux). The animals had free access to food and water. Animal experiments were performed in accordance with the guidelines published in the National Institutes of Health Guide for the Care and Use of Laboratory Animals and approved by the local IACUC committee.

2.2. Fluid percussion injury and EEG/EMG sleep-wake recordings

Fluid percussion injury in combination with EEG/EMG implantation in mice ($n=12$) was performed as previously described⁷. Mice were divided into two groups: TBI (surgery and fluid percussion injury) and sham. The fluid percussion brain injury (FPI) protocol was carried out over two days as previously described⁷. Briefly, a craniectomy was performed with a trephine (3-mm outer diameter) over the right parietal area between bregma and lambda, just medial to the sagittal suture and lateral to the lateral cranial ridge. The dura remained intact throughout the craniotomy procedure. A rigid Luer-loc needle hub (3-mm inside diameter) was secured to the skull over the opening with Loctite adhesive and subsequently cyanoacrylate plus dental acrylic. The next day, the animal was briefly placed under isoflurane anesthesia (500 mL/min) via nose cone, and respiration was visually monitored. When the animal was breathing once per two seconds, the nose cone was removed, the cap over the hub removed, and dural integrity visually confirmed. The hub was topped off with isotonic sterile saline, and a 32-cm section of high-pressure tubing extending from the FPI device attached to the Luer-loc fitting of the hub (Department of Biomedical Engineering, Virginia Commonwealth University, Richmond, VA). The animal was then placed on its left side and observed. Once normal breathing resumed and just as the animal

regained its toe pinch withdrawal reflex, a 20-ms pulse of saline onto the dura was delivered. A pressure gauge attached to an oscilloscope was used to ensure delivered pressures between 1.4 and 2.1 atmospheres, which have been previously shown to generate a mild brain injury^{13, 27, 28}. Immediately after injury, the hub was removed from the skull and the animal was placed in a supine position. The animal was then reanesthetized with isoflurane for scalp closure. Sham animals received all of the above, with the exception of the fluid pulse. The animal was returned to a heating pad until ambulatory and then returned to the home cage.

After five days of recovery, mice were connected to lightweight recording cables in individual cages. Sleep recordings were initiated after 24 hours of acclimation to the cables and continued for five days. Baseline sleep was analyzed on the first and fifth days to ensure stable sleep/wake activity across days. Therefore, the fifth day of recording corresponded to post-TBI day 13. On recording day four, mice were sleep deprived using gentle handling for three hours, from 10:00 am to 13:00 pm (Zeitgeber Time, or ZT4-6), which is a time of heightened sleep pressure in mice. Gentle handling was accomplished by providing the mice with materials such as bedding, nestlets, pieces of paper towels, aluminum foil, and saran wrap, and occasionally stroking the mice with a soft paintbrush, as previously described⁷. During this enforced wakefulness, wake was electrographically confirmed using a combination of EEG and electromyographic (EMG) signals during the entire three-hour period. An experimental timeline is provided in Figure 1.

2.3. Human subjects

Normal Group—The source of the data for this cohort consisted of polysomnography (PSG) records from a previous research study where polysomnography data (including EEG) were obtained from subjects without documented sleep disorders, as well as patients with varying degrees of obstructive sleep apnea (NIH 1R43HL076986-01A1). Following IRB approval and obtaining informed consent, each subject underwent a sleep study at the General Clinical Research Center (GCRC) of Case Western Reserve University (located within the facilities of University Hospitals of Cleveland, UHOC). PSG studies were performed according to standard clinical practices that included the attachment of bio-potential and physiological surface electrodes/sensors such as EEG (electroencephalogram), EOG (electrooculogram), EMG (electromyogram), ECG (electrocardiogram), as well as respiratory sensors (airflow) and pulse oximetry. Following the conclusion of the study, sleep staging was manually performed by a certified PSG technician, based on visual observation of the EEG, EOG, and chin EMG for each 30-second epoch duration, according to the standard clinical criteria (American Academy of Sleep Medicine (AASM)²⁹), and again confirmed by a second independent scorer (MM). The PSG records and the corresponding sleep staging of eight male and female subjects with apnea-hypopnea index (AHI) of <5 respiratory events/hour (considered clinically in the normal range) were randomly selected to represent the normal group. The average age of these subjects was 32 years old.

Mild TBI—The source of the data for this group consisted of PSG records from Veterans with mTBI admitted to an inpatient rehabilitation program at the Tampa VA. mTBI was

diagnosed by a neuropsychologist according to standard clinical criteria according to the USA Department of Veterans Affairs (2009). The 3-week program encompassed a comprehensive individualized evaluation of physical, cognitive, and mental health symptoms. The treatment phase of the program provided intensive therapy for post deployment/combat related injuries encompassing both physical and mental health symptoms. Among the evaluation and treatment protocols, and by recommendation of the sleep medicine staff, a number of these individuals were referred to the hospital's sleep laboratory for a comprehensive sleep evaluation. Overnight polysomnography was administered by certified sleep laboratory staff, and included the standard sleep montage EEG with bio-potential and physiological surface electrodes/sensors such as EEG, EOG, EMG, ECG, as well as respiratory sensors (airflow) and finger pulse oximetry. Following the conclusion of the study, standard sleep staging analysis was manually performed by a certified PSG technician, based on visual observation of the EEG, EOG, and chin EMG for each 30-second epoch duration, according to AASM criteria, and confirmed by a second independent scorer (MM). Human subjects with mTBI were on average 32 years old, 58.3 months out from their injuries at the time of their polysomnography (range, 8 to 106 months), and displayed other relevant characteristics as shown in Table 1. All mTBI subjects were assessed by a licensed neuropsychologist at the Tampa VA (TK). All subjects met criteria for chronic mTBI. There were no significant differences in outcome (i.e., Neurobehavioral Symptom Inventory scale scores) as a result of time interval from injury. Other studies have focused on QEEG in chronic TBI with similar time intervals since injury³⁰. PSG conditions were identical between groups and lasted the standard length of a typical sleep study, e.g. approximately from 22:00 to 06:00 (8 hour duration of recordings).

Retrospective analysis of PSG records was performed under IRB approval (#Pro00003124) from University of South Florida and Tampa VA. Eight consecutive male subjects with mTBI were identified who underwent diagnostic PSG and whose respiratory events were in the range not to require treatment for sleep apnea (i.e., they were not initiated onto continuous positive airway pressure therapy). Of these, 4 of 8 had an apnea-hypopnea index (AHI) > 5 events per hour. De-identified EEG channel recordings from each of the 8 subjects' PSG tests were further analyzed in MATLAB. Sleep stages included in analyses were Wake, NREM stage N1, and NREM stage N2. NREM stage N3 and REM were not included, as not every subject had these stages during the PSG recording.

Individuals with mTBI underwent the Neurobehavioral Symptom Inventory (NSI) scale, which is used within the Veterans Affairs (VA) system. The NSI is a validated, self-report measure of symptoms commonly associated with Post-Concussion Syndrome³¹. The NSI consists of 22 items or symptoms, and patients are asked to rate the degree by which each of the 22 symptoms has affected their daily functioning on a Likert Scale (0 = None, 1= Mild, 2=Moderate, 3=Severe, 4=Very Severe). NSI scores are then calculated for each of the 4 domains, Physical ('Somatic'), Cognitive, Affective and Sensory ('Vestibular'), and tallied for a total NSI score.

2.4. Data analysis: EEG and sleep/wake scoring

For mouse studies, polygraphic records were scored offline by an experienced and blinded scorer for non-rapid-eye movement (NREM) and rapid-eye-movement (REM) sleep and wakefulness (W) in 4-second epochs across the five days of recording as previously described⁷. A separate algorithm for artifact removal was applied post-hoc to raw continuous EEG data as described below.

Human PSG studies were scored by a blinded, certified PSG technician, and staging was again confirmed by an independent scorer (MM) (as described in Section 2.1).

2.5. Data analysis: EEG spectral analysis

Each EEG file associated with mouse and human PSG records underwent spectral analysis that computed the power spectral density for each channel using Welch's averaged, modified periodogram method (MATLAB, Mathworks, Inc.). The EEG records were divided into four-second segments (overlapped by one second), where each four-second segment was windowed with a Hamming window and power spectral density computed with a resolution of 0.25 Hz. From the power spectral density of each segment, the average power was computed for the following frequency bands: Delta (δ): 1–3.5 Hz; Theta (θ): 4–7.5 Hz; Alpha (α): 8–12 Hz; Sigma (σ): 13–16 Hz; Beta (β): 16.5–25 Hz; and Gamma (γ): 30–35 Hz.

For mouse files, wake epochs were used from ZT13.5 to ZT 15.5 (the two-hour period of most heightened wakefulness, at lights-off). For human subjects files, because these were overnight PSG files, wake epochs were used from the first 60 seconds of the start of recording from the central electrode (C3) and compared to state N2 NREM sleep (also from C3).

2.6. Data analysis: EEG slow wave analysis

For the mouse studies, each EEG file for a given mouse underwent a series of post-processing steps involving artifact removal, signal filtering and frequency bandwidth isolation as follows (see Figure 2 for illustration):

First, artifact removal was accomplished by detecting 'clipping' events, defined as 15 raw EEG samples (~ 60 ms) in a row being within 55 units of the amplifier maximum (or minimum). The unit is about 1/4000 of the maximum signal range on the 12-bit recorder utilized in the experiments. Each clipping event, such as shown in Figure 2A, was used to invalidate a corresponding 4-s epoch. The number of such epochs varied across the mice, but never exceeded 7% of all epochs, whereas the average fraction of invalidated epochs was about 1%. However, the removal of such epochs was essential, since the subsequent analysis focused on high-amplitude events representing less than 1% of all the epochs.

Second, a moving average of three data samples was applied to the recorded signal to smooth out any extremely high frequency spikes, as previously described¹⁶. The three data sample moving average filter applied at the sampling frequency of 256 Hz is equivalent to removing frequencies greater than 80Hz (i.e., far outside the frequency band of interest between 1 to 8 Hz).

Third, a basic Fermi window function $f(n) = \left(1 + e^{5 - \frac{n}{50}}\right)^{-1}$, where n is the sample number, was applied as a multiplicative correction to gradually attenuate the first two seconds (512 samples) of each recorded signal, a negligible amount of data from the 3- to 24-hour analysis files. However, without this windowing, a ringing artifact was observed with the application of the Butterworth Filter (see next step) due to the discontinuous nature of the initial data points.

The fourth step in post-processing involved isolating the 1 to 8 Hz frequency band of interest by numerically applying a 4th order Butterworth band-pass filter (see Figure 2C). The frequency range of 1 to 8 Hz was chosen because of its non-overlap with traditional waking EEG frequencies in the alpha range (9–13 Hz) and higher. This range has been applied to human sleep EEG data before for the quantification of slow waves in local sleep¹⁶. The Butterworth Filter was chosen primarily for its flatness of the amplitude response within the pass band. Signal amplitude is a characteristic that is vital to our subsequent stages of peak quantification (see next steps, and validation in Figure 2E–H).

Subsequent post-processing steps include the following: The resulting filtered data signal from each mouse was analyzed for negative troughs in the EEG signal using modifications to methods previously described¹⁶. Positive transients show downwards whereas negative transients go up. First, zero crossings were located and the absolute minima between each pair of consecutive zero crossings were identified (thereby avoiding inadvertent quantification of multiple local minima of the same trough) for NREM and wake states for each individual mouse. Values of the filtered signal amplitude at the minima for NREM and wake states were then normalized to the median value of such minimal amplitudes during REM sleep during the previous hour (for the 3-hr data set) or the first 12 hours (of the 24-hr data set) for each individual mouse. Unlike human sleep data, individual normalization is necessary in animal studies due to the individual differences between mice in hardware, impedance, amplification and gain of each recording. The ideal normalization factor is an immutable constant. REM sleep was chosen as the baseline for normalization for several reasons. In mice, REM is relatively monochromatic (i.e. a single frequency, usually 7–8 Hz and constant within an individual animal), and the amplitude remains fairly constant and consistent within a single animal across our 5 days of recording. In contrast, NREM, wake, and total power all change with varying conditions (i.e., light or dark, sleep deprivation or recovery sleep). Thus, the amplitudes during REM sleep are the best representation of the signal strength of the whole brain of the mouse, and therefore it is an ideal factor with which to normalize prior to comparing slow wave counts against other mice. Also, the percentage of REM sleep does not significantly differ between TBI and sham mice⁷, and predominant EEG frequencies in REM sleep in the theta range (5–8 Hz) are included within our frequency analysis range of 1 to 8 Hz.

Based on REM sleep of the individual animal, we next set a relative voltage threshold above which to count slow waves. Any metric that is based on median or average (e.g., the 50th percentile) will likely capture a significant amount of noise or random events in addition to the signal of interest (e.g., slow waves). Here, we attempt to identify rare slow wave events with the deepest minima, which are concentrated within the tail of a given distribution. In

our simulated data model, in which EEG data for six ‘mice’ was created using independent random signal values from a Gaussian distribution, a threshold set at three times the median amplitude of minima during REM sleep was applied (see Figure 2G). This threshold was high enough to remove most noise, but still low enough to capture enough of the deepest slow waves to be meaningful. The purpose of generating the simulated data (essentially a dataset of random numbers) was to establish a benchmark for the number of rare events that are detected that are due to chance; therefore, the 3x cutoff falls within the desired balance of signal:noise.

All mice in the study experienced at least 50 epochs of REM sleep (and on average, over 150 epochs) during the 1-hour baseline period from 09:00 to 10:00 on recording Day 4. Using the simulated data as a guide, a threshold value for the physiological data was set at three times the median amplitude of the minima quantified during REM sleep for each mouse, and only the values exceeding the threshold (i.e., the deepest minima) for each mouse were counted as slow waves (see Figure 2H). Only the deepest minima were counted because previous work has established that slow waves with the deepest minima correspond to longer periods of cortical silence from larger groups of neurons^{32,33}.

EEG slow wave counts were analyzed from the following periods for each mouse: 1) over 24 hours of spontaneous NREM sleep (07:00 to 07:00), 2) over 24 hours of spontaneous wakefulness (07:00 to 07:00), and 3) experimentally-enforced wakefulness (10:00 am to 13:00 pm).

For EEG from human subjects, the same method as described above was employed for detection of negative troughs within the frequency range specified for mice. It again should be noted that in human EEG, normalization is not necessary due to standardization of scalp electrodes and use of absolute voltage scales. Therefore, for human EEG wave counts, voltages were not normalized, and a percentage threshold (75th percentile and above) was applied above which slow waves were selected for analysis. This percentage threshold approach is similar to what has been done previously for human EEG slow wave counts¹⁶. As these were attended overnight studies performed in an AASM-accredited sleep laboratory, EEG-related artifacts were usually immediately corrected by the sleep technician, thus minimizing the number of EEG-related artifacts. Furthermore, within the analyzed PSG records, the slow wave algorithm that was applied rejected the slow waves in which the magnitude exceeded the threshold set for artifact (‘clipped’ traces).

Determination of the threshold (values below which a trough was counted as a ‘slow wave’) was based on the 75th percentile of all negative troughs from each individual’s awake data¹⁶.

2.7. Data analysis: Global Coherence Index

A measure of co-occurrence of slow waves among the bi-hemispheric occipital and central EEG channels was defined and applied to the human data. This ‘Global Coherence Index’ was based on relative time of occurrences of slow waves in each EEG channel and was computed as follows: For each wake and sleep state, consecutive time intervals of 0.1 second duration (bins) were defined, and the occurrence of slow wave peaks in each EEG channel was marked as either 1 (if a slow wave peak appeared in that bin) or zero (no slow wave

peak occurred). This was followed by summing the counts for all four channels (O1, O2, C3, C4) for every bin resulting in a number ranging from 0 (no peaks in any channels) to 4 (all four EEG channels had a peak). Subsequently, each bin was assigned the value 1 if there were either no peaks in the bin or all four channels had peaks, or assigned the value 0 if there were 1, 2, or 3 peaks present. These 0 or 1 values then were averaged across the 600 bins (each bin was 0.1 seconds, with 60 seconds analyzed in total), and converted to percentages.

2.8. Statistical procedures

As there have been no prior publications performing this type of EEG individual slow wave quantification in human subjects with TBI, sample sizes for the human subjects studies were determined using power analyses based on the data from our preliminary experiments using mice. Our mouse data comparing TBI with sham control mice during wakefulness showed a Cohen's effect size of 1.9, based on the difference of the mean values of the theta-alpha ratios, divided by the square root of the mean of the variances of the two groups. Using a power level of 0.9 and an alpha probability of 0.05, our minimum sample size for a two-tailed t-test is $n=7$ per group. We thus analyzed $n=8$ human subject with TBI and $n=8$ age-matched control subjects.

Statistical calculations and analyzes were performed using the open-source program R (Version 2.15.2, The R Foundation of Statistical Computing)³⁴ and MATLAB (MathWorks, Inc.). Where appropriate, all data were analyzed using Two-way ANOVA, Student's t-tests and Pearson's correlations. Statistical significance was defined at the $p < 0.05$ confidence level when comparing different treatment groups. In the case of multiple (>4) comparisons (i.e., cross-frequency coupling analyses), Bonferroni corrections were applied to the p -value cutoff for significance. All data are presented as group means \pm SEM.

3. Results

3.1. EEG Amplitude Analyses

In order to quantify the EEG-based changes in sleep and wakefulness after TBI, we first examined EEG amplitudes by computing spectral power across frequency bands during sleep and wakefulness in mice after either fluid percussion injury or sham control injury. EEG amplitudes were then examined as a ratio between two different frequency band pairs.

During the awake state, the theta:alpha amplitude ratio was significantly higher in TBI compared to sham-injured mice ($p=0.0095$, $t=10.79$, Student's t-test with significance set at $p < 0.01$ based on Bonferroni adjustment for multiple comparisons) (Figure 3A and 3B). During NREM sleep, the theta:alpha amplitude ratio was not significantly different ($p=0.023$, $t=7.49$, Student's t-test with significance set at $p < 0.01$ based on Bonferroni adjustment for multiple comparisons) (Figure 3C), nor were any other frequency band pair combinations significantly different between groups (data not shown).

Next, we applied the same amplitude ratio analysis to sleep-wake EEG from human subjects after mTBI. Unlike mice, theta:alpha amplitude ratio did not significantly differ between groups during the awake state ($p=0.79$, $t=0.27$, Student's t-test). However, mTBI patients did

show significantly increased theta:beta amplitude ratio while awake ($p=0.00005$, $t=33.73$, Student's t-test with significance set at $p<0.01$ based on Bonferroni adjustment for multiple comparisons) (Figure 3D and 3E). In contrast, during NREM sleep, the theta:beta amplitude ratio did not significantly differ between groups ($p=0.11$, $t=2.82$, Student's t-test) (Figure 3F), nor were any other frequency band pair combinations significantly different between groups (data not shown).

Taken together, both mouse and human spectral analyses indicate that theta amplitude, coupled to faster frequencies such as alpha (mouse) or beta (human) amplitudes, is increased after brain injury and particularly during wakefulness.

3.2. EEG slow wave counts during sleep and wake states in mice

Next, we applied our method for EEG slow wave quantification to EEG from brain-injured and sham-injured mice. During a 24-hour period of continuous EEG recording of baseline sleep-wake states, slow wave counts were calculated for each 30 minute bin, corrected for individual differences in the relative amounts of NREM or wake states per bin, and then plotted as group averages superimposed upon percentage time spent in NREM or wake states (Figure 4A and 4B for wake, and Figure 5A and 5B for NREM).

During spontaneous wakefulness, TBI mice showed significantly more EEG slow waves compared to sham control mice, particularly during the dark phase when mice are typically more awake ($p=0.02$, $t=2.809$, Student's t-test) (Figure 4C). Sham control and TBI mice did not significantly differ in the total amounts of EEG slow waves during spontaneous NREM sleep ($p>0.05$, $t=1.701$, Student's t-test) (Figure 5C). These data indicate that the increase in EEG slow waves after TBI is particularly salient during the awake state.

3.3. EEG slow wave counts during enforced wakefulness in mice

Given the results above showing that brain injury results in increased EEG slow waves during spontaneous wakefulness, we next sought to determine whether EEG slow waves could be modulated by cumulative time spent awake. Mice were sleep-deprived for a three-hour period from 10:00 to 13:00 (or Zeitgeber Time ZT4-6), a period of heightened sleep pressure. A three-hour time period was chosen because typically, naïve and sham control mice do not show significant sleep rebound of either NREM or REM sleep after just 3 hours of enforced wakefulness^{7,35}.

Brain-injured mice showed significantly increased slow wave counts during the third consecutive hour of sleep deprivation compared to sham-injured mice ($p=0.0060$, $F(3,1419)=5.156$, two-way ANOVA; $p<0.05$, $t=2.691$, Bonferroni post-hoc test for Hour 3) (Figure 4D). These data suggest that EEG slow waves can be modulated by prior waking history, and accumulate faster in the brain-injured mice during sustained wakefulness compared to the uninjured brain, possibly reflecting injury-induced changes in the sleep homeostat.

3.5. EEG slow wave counts during sleep and wake states in human subjects

Given the results showing that brain injury in mice results in a state-dependent increase in EEG slow waves during wakefulness, and that these EEG slow waves are modulated by prior waking experience, we next sought to determine whether human subjects with mTBI also showed more EEG slow waves while awake.

Compared to age-matched control subjects, brain-injured human subjects showed significantly more EEG slow waves during wakefulness ($p < 0.0001$, $F = 117.5$, two-way ANOVA; $p < 0.001$, $t = 6.54, 5.29, 5.73, 4.12$, Bonferroni post-hoc tests for C3, C4, O1 and O2, respectively) (Figure 6A). Also similar to mice, there was no significant difference in EEG slow wave counts between groups in NREM stage N1 sleep ($p > 0.05$, $F = 2.34$, two-way ANOVA; $p > 0.05$, Bonferroni post-hoc tests) or NREM stage N2 sleep ($p < 0.01$, $F = 11.97$, two-way ANOVA; $p > 0.05$, Bonferroni post-hoc tests) (Figure 6B and 6C). These data indicate that again, similar to mice, human TBI is associated with an increase in EEG slow waves during wakefulness.

Next, we generated traditional power spectral plots comparing mTBI with control subjects for wake and NREM stage N2 sleep (Supplemental Figure 1). The increased power density between 2–9 Hz range during wakefulness (but less so during NREM sleep) in subjects with mTBI is consistent with findings from our novel method of quantifying individual slow waves.

Sleep staging is in part defined by an increase in EEG slow waves during the transition from wake to NREM stage N1, and from N1 to N2 sleep (AASM,²⁹). We compared the difference in slow waves between sleep and wakefulness in mTBI and control subjects. Control subjects showed the expected increase in EEG slow waves in NREM stage N1 sleep compared to wakefulness, whereas this increase was completely absent in TBI subjects ($p < 0.0001$, $F = 40.70$, two-way ANOVA; $p < 0.01$, $p > 0.05$, $p < 0.01$, $p < 0.05$, $t = 3.88, 2.47, 3.66, 2.75$, Bonferroni post-hoc tests for C3, C4, O1 and O2, respectively) (Figure 6D). Similarly, control subjects showed the expected increase in EEG slow waves in NREM stage N2 sleep compared to wakefulness, whereas this increase was significantly smaller in TBI subjects ($p < 0.0001$, $F = 60.33$, two-way ANOVA; $t = 4.36, 3.41, 4.47, 3.30$, $p < 0.001$, $p < 0.01$, $p < 0.001$, $p < 0.01$, Bonferroni post-hoc tests for C3, C4, O1 and O2, respectively) (Figure 6E). Taken together, these data suggest that mTBI is associated with less of a distinction between sleep and wake states, perhaps contributing to a blurring of sleep and wakefulness. A complementary explanation is that mTBI is associated with disruption in the local sleep homeostat.

3.6. Global coherence of EEG slow waves in human subjects

In order to assess the degree of EEG synchrony of slow waves across channels in mTBI, we compared the Global Coherence Index across wake and NREM stage N2 sleep in human subjects with mTBI and age-matched controls. Individual EEG slow waves during wake and N2 sleep were plotted over time on a Raster plot, akin to that typically used for spike timing in neuronal firing (Figure 7A and 7C). The Global Coherence Index (represented as the percentage of time spent with either 0 or 4 EEG slow waves across channels) was

significantly lower in mTBI subjects compared to controls while awake (Figure 7B; $p=0.000008$, $t=6.81$, Student's *t*-test). Groups did not significantly differ in their Global Coherence Index during N2 sleep (Figure 7D; $p=0.54$, $t=0.62$, Student's *t*-test). Next, the Global Coherence Index for each individual subject with mTBI was correlated with TBI symptom severity as assessed by the self-reported Neurobehavioral Symptom Inventory (NSI) scale. Higher coherence indices strongly predicted more severe symptoms reported on the NSI (Pearson's $r=0.84$, $R^2=0.71$, $p=0.0086$) (Figure 7E). The four subcomponents of the NSI (Vestibular, Somatic, Cognitive and Affective) were each correlated with the Synchrony Index from each individual with mTBI. Each subcomponent resulted in a strong positive correlation, with the Cognitive component being the strongest contributor (Pearson's $r=0.49, 0.64, 0.73$, and 0.59 , respectively). No significant correlations existed for stage N2 sleep (overall NSI: Pearson's $r=-0.19$, $R^2=0.036$, $p=0.65$) (Figure 7F).

Taken together, these data suggest that individuals with mTBI have less temporal coherence of EEG slow waves while awake. The degree of EEG slow wave coherence in mTBI while awake strongly predicts symptom severity.

In summary, our data show that EEG slow waves can be objectively quantified in the injured brain using quantitative EEG. Both mouse and human subjects with mTBI showed an increase in EEG slow waves during wakefulness. Mice with mTBI showed greater accumulation of slow waves the longer they stayed awake. Human subjects with mTBI showed less EEG coherence of slow waves while awake, and the degree of coherence correlated with symptom severity. These data suggest that the presence of EEG slow waves may reflect a novel, relatively specific, sleep-related feature of brain dysfunction in mTBI.

4. Discussion

Our studies in both mouse and human subjects with mTBI establish an objective, automated method to quantify the number and global coherence of EEG slow waves during sleep and wake states, and show that mTBI is associated with significantly increased quantity and decreased global coherence of EEG slow wave counts during wakefulness. Taken together, our data suggests that EEG slow waves and desynchrony of slow waves across channels could represent dysregulation of the homeostat of sleep and wakefulness after mTBI.

While other groups have applied quantitative EEG (QEEG) approaches to understanding the physiology of brain injury, these approaches have largely relied on spectral power analyses averaged over a short time period of EEG recording in the acute phase post-TBI^{24,30,36-38}. QEEG analyses during both sleep and wakefulness is important given the strong association between TBI and sleep disturbances, and the apparent interference of such sleep disturbances with rehabilitation contributing to long-term disability^{11,39-41}. One QEEG study using human subjects after sports-related concussions within the past 12 months found that concussions were associated with an increase in delta power and a reduction in alpha power in the waking EEG, without significant changes in the sleep EEG²⁶. We applied a novel method of counting individual slow waves and calculated a coherence index of slow waves across multiple channels that showed an intrusion of sleep-like EEG frequencies during normal wakefulness in subjects with mTBI. Furthermore, our data lends support to

recent findings by others that the number of EEG slow waves can be modulated by prior waking activity, and may be consistent with the phenomenon of “local sleep” which displays sleep-like activity on the spectrum of wakefulness to sleep¹⁷. While the mechanism remains unclear, decreased global coherence of slow waves seen in mTBI is consistent with greater local sleep in the injured brain.

Prior studies of sleep and wakefulness have proposed the idea of local, use-dependent sleep as a property of bottom-up neural networks, in essence placing sleep and wakefulness on two ends of the same overlapping spectrum^{42,43}. In accordance with this, it was recently reported that EEG frequencies in the 1 to 8 Hz range, which are traditionally seen during sleep, may intrude into normal waking EEG frequencies during prolonged wakefulness in rodents, a phenomenon known as ‘local sleep’¹⁷. Rats showing more slow waves during wakefulness had more errors in behavioral performance, indicating a functional consequence to this phenomenon¹⁷. Similar reports of slower EEG frequencies during prolonged wakefulness have also been reported in humans¹⁶. Recent evidence shows that TBI itself may also affect local neural networks in a controlled cortical impact model of rodent TBI⁴⁴. High-speed biosensor imaging showed glutamate signaling was increased in the injured cortex, and GABAergic interneuron immunoreactivity was decreased throughout the injured cortex⁴⁴. Thus, it is possible that the neurochemical correlate of increased glutamate and decreased GABA may affect neuronal energetics in a way that leads to local neuronal silencing and local EEG slow waves. We hope that our method for quantifying individual slow waves and calculating a phase-based global coherence of slow waves might be relevant for future studies examining local sleep during wakefulness.

In our studies, mTBI in mice and humans showed several interesting parallels, including persistent sleep disturbances, the inability to maintain wakefulness, and in the current study, more slow waves during wakefulness^{7, 45}. However, in the current study, there were also notable species differences. For example, mice with TBI showed differences in theta:alpha ratios, whereas human subjects with mTBI showed differences in theta:beta ratios. While theta rhythm itself may be important in distinguishing injured from non-injured brain, depending on the species, there may be different coupling to slower (e.g., alpha for mouse) versus faster frequencies (e.g. beta for human).

It is worth discussing several caveats related to our findings. First, the fluid percussion injury model in rodents, while widely accepted and used worldwide for over 3 decades, lacks the acceleration/deceleration mechanisms that may impact brainstem structures (including sleep regulatory regions) seen in human TBI. However, the fact that EEG slow waves are increased in both rodent and human models is compelling evidence that they may share the same underlying pathophysiological mechanisms. Secondly, EEG slow waves are often seen with epileptiform spike-and-wave morphology; therefore, EEG slow waves associated with sleep homeostasis must be distinguished from the epileptiform activity frequently observed in post-traumatic epilepsy. We manually reviewed each EEG record for epileptiform abnormalities, and excluded these in the final analysis (only 1 mouse showed seizure activity; no human subjects showed epileptiform activity). Thirdly, our mTBI cohort was selected from a group undergoing active rehabilitation, which may carry inherent selection bias compared to those not under active rehabilitation. Fourthly, human subjects in our

studies did not consistently show NREM stage N3 or REM sleep, possibly reflecting a “first-night effect,” and our sampling was limited to central and occipital rather than frontal leads, thus decreasing the ability to detect group differences within the sleep EEG. Fifthly, in human neurophysiology studies, EEG slowing is often viewed as a nonspecific sign of cerebral dysfunction, as focal EEG slowing may be observed specifically over an area with a structural lesion^{46,47}. However, the vast majority of patients with mTBI (including in our cohort) have no known structural lesion and normal neuroimaging. Focal EEG slowing is typically found in the same electrode or localized set of electrodes. We observed EEG slow wave intrusion into the waking EEG across several bihemispheric electrodes in both normal control subjects as well as those with mTBI and OSA. Furthermore, our finding that sleep deprivation increases the frequency of EEG slow waves implies a state-dependent modulation of this phenomenon. Thus, we propose that EEG slowing in mTBI patients is mechanistically different from focal EEG slowing in epilepsy/ encephalopathy, and may represent ‘local sleep’ – a use-dependent property of local cortical neurons, and a potential indicator of increased sleepiness on the spectrum of prolonged wakefulness. However, more research into the neuronal activity and mechanisms underlying EEG slow waves in TBI is warranted.

In our study, subjects with mTBI showed significantly shorter sleep latencies compared to age-matched control subjects (Table 1), consistent with a well-described phenotype of excessive daytime sleepiness. Other studies have suggested there may be a higher prevalence of sleep disorders in people with TBI, and indeed, in our cohort of TBI subjects, a few did meet criteria for mild OSA on the basis of the apnea-hypopnea index (AHI between 5 to 15)⁴⁸. It is possible that mild OSA could contribute to the EEG findings in patients with mTBI, although patients with more severe sleep apnea do not have increased EEG slow waves (see Supplemental Material). It is also possible that our findings could in part reflect other common comorbidities in mTBI, such as post-traumatic stress disorder (PTSD), which also affects sleep⁴⁹. It is likely that EEG slow waves are directly relevant to mTBI, because this finding was observed in our highly controlled animal model of mTBI (a model which does not include comorbid PTSD or OSA), and then later confirmed in human subjects with mTBI. The strength of our translational approach not only provides an additional screening layer to the identification of promising biomarkers, but will also allow us to return to the animal model to dissect the underlying mechanisms of EEG slow waves in brain injury, and more importantly, develop ways to experimentally manipulate EEG slow waves and global coherence as a potential treatment.

Subjects with mTBI on average showed less EEG coherence while awake compared to age-matched control subjects, yet those mTBI subjects with the least EEG coherence had the mildest symptoms as reported on the NSI. It is possible that this positive correlation could reflect the tendency of those with the most severe symptoms to have more microsleep episodes, a phenomenon in which the whole brain undergoes a brief, synchronous sleep episode lasting milliseconds to seconds. This finding warrants further analyses in future studies.

A subset of patients with chronic mTBI experiences persistent post-concussive symptoms that are often severely debilitating, for whom there are no reliable diagnostic or prognostic

indicators. The number and/or global coherence of EEG slow waves during clinical EEG studies, either in short form (i.e., routine EEG for 20 minutes), or extended polysomnography, both of which are readily clinically available, could represent a metric to potentially diagnose and/or predict who will go on to experience post-concussive disability, and provide earlier, targeted interventions as appropriate. Future studies should examine other outcome measures in relation to the EEG, as well as apply longitudinal follow-up.

Supplementary Material

Refer to Web version on PubMed Central for supplementary material.

Acknowledgments

This material is the result of work supported with resources and the use of facilities at the VA Portland Health Care System, the VA Career Development Award # IK2 BX002712, the American Sleep Medicine Foundation, and the Portland VA Research Foundation (MML). This material is also supported by VA RR&D Brain Rehabilitation Research Center grant B9256-C and NIH #1R43HL076986-01A1 (MM). The contents do not represent the views of the U.S. Department of Veterans Affairs or the United States Government.

References

1. Baumann CR, et al. Sleep-wake disturbances 6 months after traumatic brain injury: a prospective study. *Brain*. 2007; 130:1873–1883. [PubMed: 17584779]
2. Kempf J, et al. Sleep-wake disturbances 3 years after traumatic brain injury. *J Neurol Neurosurg Psychiatry*. 2010; 81:1402–1405. [PubMed: 20884672]
3. Makley MJ, et al. Prevalence of sleep disturbance in closed head injury patients in a rehabilitation unit. *Neurorehabil Neural Repair*. 2008; 22:341–347. [PubMed: 18663247]
4. Makley MJ, et al. Return of memory and sleep efficiency following moderate to severe closed head injury. *Neurorehabil Neural Repair*. 2009; 23:320–326. [PubMed: 19171947]
5. Kimura A, et al. A minor high-molecular-weight outer membrane protein of *Haemophilus influenzae* type b is a protective antigen. *Infect Immun*. 1985; 47:253–259. [PubMed: 2578121]
6. Mollaveya T, et al. The Risk of Sleep Disorder Among Persons with Mild Traumatic Brain Injury. *Curr Neurol Neurosci Rep*. 2016; 16:55. [PubMed: 27079955]
7. Lim MM, et al. Dietary therapy mitigates persistent wake deficits caused by mild traumatic brain injury. *Sci Transl Med*. 2013; 5:215ra173.
8. Lim MM, et al. Controlled cortical impact traumatic brain injury acutely disrupts wakefulness and extracellular orexin dynamics as determined by intracerebral microdialysis in mice. *J Neurotrauma*. 2012; 29:1908–1921. [PubMed: 22607167]
9. Rowe RK, et al. Recovery of neurological function despite immediate sleep disruption following diffuse brain injury in the mouse: clinical relevance to medically untreated concussion. *Sleep*. 2014; 37:743–752. [PubMed: 24899763]
10. Skopin MD, et al. Chronic decrease in wakefulness and disruption of sleep-wake behavior after experimental traumatic brain injury. *J Neurotrauma*. 2015; 32:289–296. [PubMed: 25242371]
11. Nakase-Richardson R, et al. Prospective evaluation of the nature, course, and impact of acute sleep abnormality after traumatic brain injury. *Arch Phys Med Rehabil*. 2013; 94:875–882. [PubMed: 23296143]
12. Dixon CE, et al. A fluid percussion model of experimental brain injury in the rat. *J Neurosurg*. 1987; 67:110–119. [PubMed: 3598659]
13. McIntosh TK, et al. Traumatic brain injury in the rat: characterization of a lateral fluid-percussion model. *Neuroscience*. 1989; 28:233–244. [PubMed: 2761692]
14. Sommerauer M, et al. Excessive sleep need following traumatic brain injury: a case-control study of 36 patients. *J Sleep Res*. 2013; 22:634–639. [PubMed: 23837871]

15. Imbach LL, et al. Increased sleep need and daytime sleepiness 6 months after traumatic brain injury: a prospective controlled clinical trial. *Brain*. 2015; 138:726–735. [PubMed: 25595147]
16. Hung CS, et al. Local experience-dependent changes in the wake EEG after prolonged wakefulness. *Sleep*. 2013; 36:59–72. [PubMed: 23288972]
17. Vyazovskiy VV, et al. Local sleep in awake rats. *Nature*. 2011; 472:443–447. [PubMed: 21525926]
18. Arbour C, et al. Are NREM sleep characteristics associated to subjective sleep complaints after mild traumatic brain injury? *Sleep Med*. 2015; 16:534–539. [PubMed: 25747335]
19. Cote KA, et al. Sleep and waking function following traumatic brain injury. *AIMS Neuroscience*. 2015; 2:203–228.
20. Khoury S, et al. Rapid EEG activity during sleep dominates in mild traumatic brain injury patients with acute pain. *J Neurotrauma*. 2013; 30:633–641. [PubMed: 23510169]
21. Parsons LC, et al. Longitudinal sleep EEG power spectral analysis studies in adolescents with minor head injury. *J Neurotrauma*. 1997; 14:549–559. [PubMed: 9300565]
22. Williams BR, et al. Polysomnographic and quantitative EEG analysis of subjects with long-term insomnia complaints associated with mild traumatic brain injury. *Clin Neurophysiol*. 2008; 119:429–438. [PubMed: 18083618]
23. Schneider E, Hubach H. The EEG in traumatic psychoses. *Dtsch Z Nervenheilkd*. 1962; 183:600–627. [PubMed: 13908910]
24. Nuwer MR, et al. Routine and quantitative EEG in mild traumatic brain injury. *Clin Neurophysiol*. 2005; 116:2001–2025. [PubMed: 16029958]
25. Courjon, J.; Scherzer, E. *Traumatic disorders*. Elsevier; 1972. p. 1-104.
26. Gosselin N, et al. Sleep following sport-related concussions. *Sleep Med*. 2009; 10:35–46. [PubMed: 18226956]
27. Dixon CE, et al. Physiologic, histopathologic, and cineradiographic characterization of a new fluid-percussion model of experimental brain injury in the rat. *J Neurotrauma*. 1988; 5:91–104. [PubMed: 3225860]
28. Carbonell WS, et al. Adaptation of the fluid percussion injury model to the mouse. *J Neurotrauma*. 1998; 15:217–229. [PubMed: 9528921]
29. The AASM Manual for the Scoring of Sleep and Associated Events: Rules, Terminology and Technical Specifications. 2014. Version 2.1
30. Leon-Carrion J, et al. Delta-alpha ratio correlates with level of recovery after neurorehabilitation in patients with acquired brain injury. *Clin Neurophysiol*. 2009; 120:1039–1045. [PubMed: 19398371]
31. Cicerone KD, Kalmar K. Persistent postconcussion syndrome: The structure of subjective complaints after mild traumatic brain injury. *J Head Trauma Rehabil*. 1995; 10:1–17.
32. Vyazovskiy VV, et al. Cortical firing and sleep homeostasis. *Neuron*. 2009; 63:865–878. [PubMed: 19778514]
33. Buzsaki G, et al. The origin of extracellular fields and currents—EEG, ECoG, LFP and spikes. *Nat Rev Neurosci*. 2012; 13:407–420. [PubMed: 22595786]
34. Team, R. C.. *R Foundation for Statistical Computing*. 2012.
35. Franken P, et al. Sleep homeostasis in the rat: simulation of the time course of EEG slow-wave activity. *Neurosci Lett*. 1991; 130:141–144. [PubMed: 1795873]
36. Watson MR, et al. The post-concussional state: neurophysiological aspects. *Br J Psychiatry*. 1995; 167:514–521. [PubMed: 8829722]
37. Leon-Carrion J, et al. Synchronization between the anterior and posterior cortex determines consciousness level in patients with traumatic brain injury (TBI). *Brain Res*. 2012; 1476:22–30. [PubMed: 22534483]
38. Leon-Carrion J, et al. A QEEG index of level of functional dependence for people sustaining acquired brain injury: the Seville Independence Index (SINDI). *Brain Inj*. 2008; 22:61–74. [PubMed: 18183510]
39. Nakase-Richardson R, et al. Prospective comparison of acute confusion severity with duration of post-traumatic amnesia in predicting employment outcome after traumatic brain injury. *J Neurol Neurosurg Psychiatry*. 2007; 78:872–876. [PubMed: 17178822]

40. Sherer M, et al. Effect of severity of post-traumatic confusion and its constituent symptoms on outcome after traumatic brain injury. *Arch Phys Med Rehabil.* 2008; 89:42–47. [PubMed: 18164329]
41. Silva MA, et al. Posttraumatic confusion predicts patient cooperation during traumatic brain injury rehabilitation. *Am J Phys Med Rehabil.* 2012; 91:890–893. [PubMed: 22660372]
42. Krueger JM, Obal F. A neuronal group theory of sleep function. *J Sleep Res.* 1993; 2:63–69. [PubMed: 10607073]
43. Krueger JM, Tononi G. Local use-dependent sleep; synthesis of the new paradigm. *Curr Top Med Chem.* 2011; 11:2490–2492. [PubMed: 21906015]
44. Cantu D, et al. Traumatic Brain Injury Increases Cortical Glutamate Network Activity by Compromising GABAergic Control. *Cereb Cortex.* 2014
45. Willie JT, et al. Controlled cortical impact traumatic brain injury acutely disrupts wakefulness and extracellular orexin dynamics as determined by intracerebral microdialysis in mice. *J Neurotrauma.* 2012; 29:1908–1921. [PubMed: 22607167]
46. Krauss, GL. *Focal and Generalized Slow Patterns.* The Johns Hopkins University Press; 2006.
47. Gloor P, et al. Brain lesions that produce delta waves in the EEG. *Neurology.* 1977; 27:326–333. [PubMed: 557774]
48. Castriotta RJ, Lai JM. Sleep disorders associated with traumatic brain injury. *Arch Phys Med Rehabil.* 2001; 82:1403–1406. [PubMed: 11588744]
49. Ross RJ, et al. Sleep disturbance as the hallmark of posttraumatic stress disorder. *Am J Psychiatry.* 1989; 146:697–707. [PubMed: 2658624]

Highlights

- Mild traumatic brain injury (mTBI) in mice is associated with more EEG slow waves during wakefulness.
- Chronic mTBI in humans is associated with more EEG slow waves during wakefulness.
- A novel metric of global coherence across multiple channels was calculated for EEG slow waves.
- Global coherence of EEG slow waves was significantly correlated with severity of post-concussive symptoms.
- Sleep EEG slow wave quantity and coherence may represent a sensitive marker of mTBI and post-concussive symptoms.

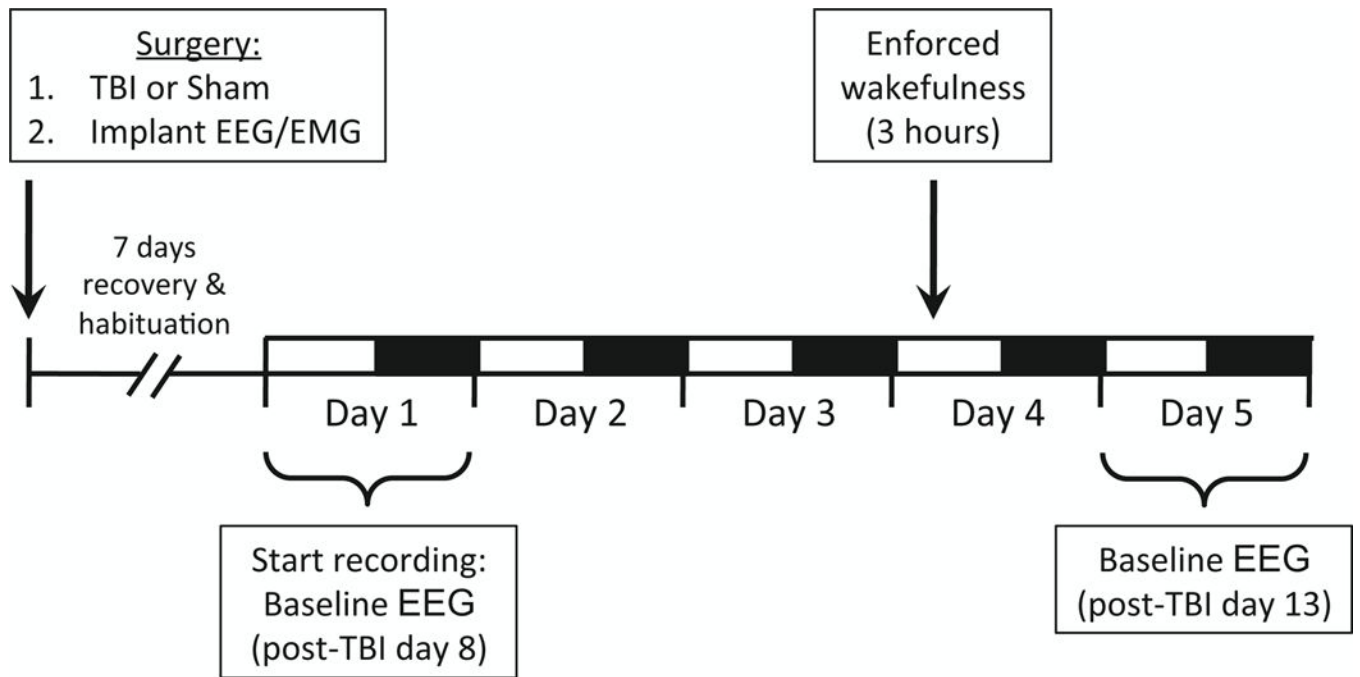


Figure 1.
Experimental timeline for mouse EEG studies.

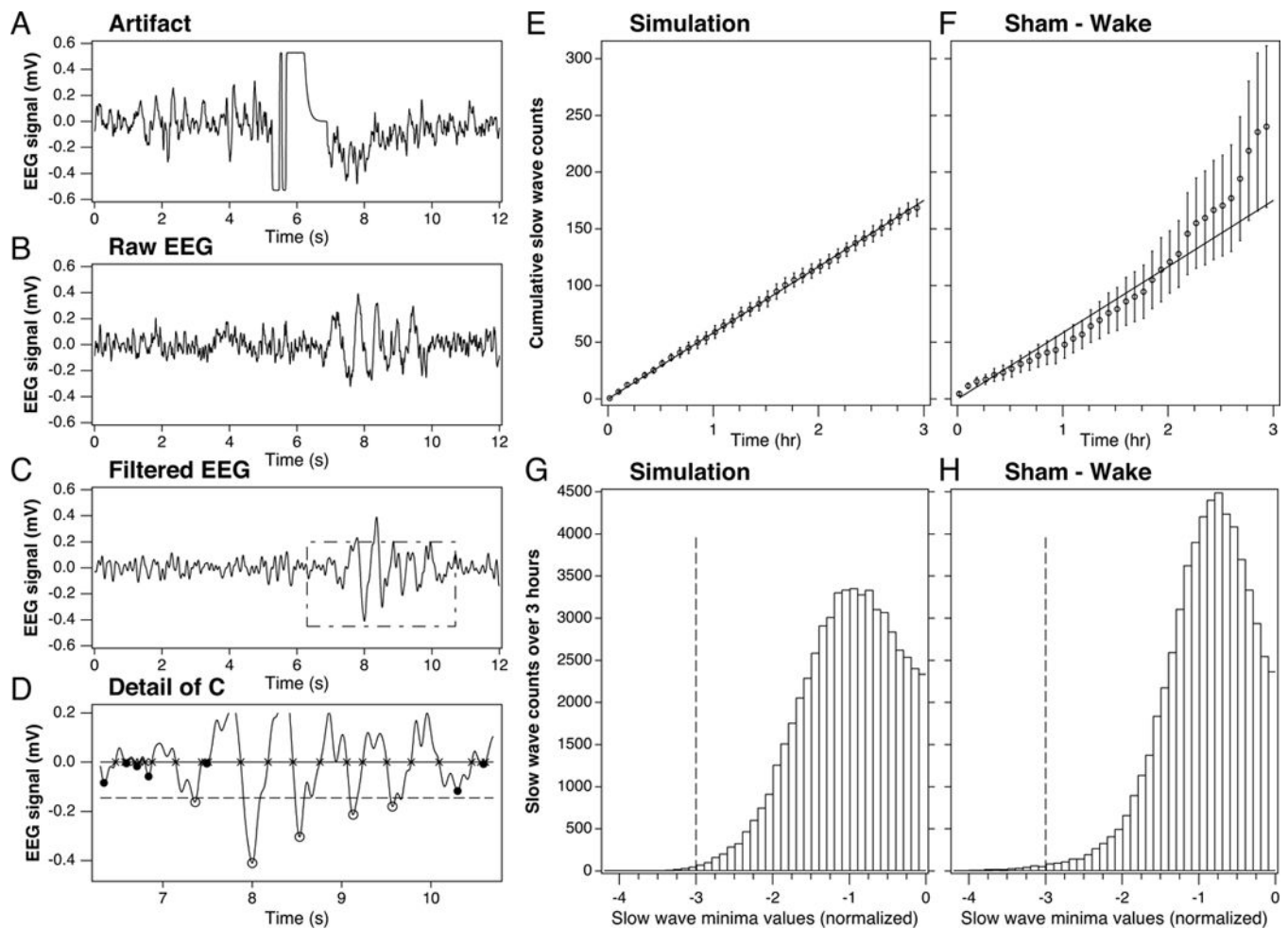


Figure 2. EEG signal post-processing steps in simulated and physiologic mouse EEG datasets

(A) Sample artifact rejection using automated algorithm designed to detect 15 consecutive samples within 55 binary units of the amplifier maximum (or minimum) from raw EEG trace. In this example, deep minima between 4 and 8 seconds would be removed from the data.

(B) Sample raw EEG trace lasting 12 seconds, or 3 epochs, from a mouse during enforced wakefulness. All epochs during enforced wakefulness were confirmed as wake on the basis of combined EEG and EMG criteria.

(C) Butterworth filter applied to the sample raw EEG trace from panel A.

(D) Identification of zero crossings (× symbols) and minima (open circles) exceeding the threshold (dashed line), set at three times the median amplitude of all minima during REM sleep.

(E) Cumulative averages of simulated slow-wave counts for $n=6$ traces generated from an uncorrelated Gaussian noise sample showing effects of post-processing steps (i.e., filters and zero crossings/minima identification) on noise alone. Data represent cumulative counts of the minima exceeding the threshold for each trace over three consecutive hours.

(F) Actual EEG data collected from sham-injured mice during 3 hours of enforced wakefulness, showing effects of post-processing steps (i.e., artifact rejection, filters, zero

crossings/ minima identification) on physiologic EEG. Note that sham control mice show a similar (but not identical) accumulation of slow wave counts compared to simulated EEG data, indicating a that high-amplitude minima in sham mice are distributed similar to those produced by random noise.

(G) Histogram of simulated EEG data of a single trace showing the distribution of minima values and the threshold (dashed line) set at three times the median amplitude of the minima during the preceding hour.

(H) Histogram of physiologic EEG data from a single sham control mouse showing the distribution of minima values and the threshold (dashed line) set at three times the median peak height during REM sleep. The amplitude bins in both histograms are normalized such that -1 indicates the median amplitude of the corresponding reference. Only minima above this threshold were included in slow wave counts.

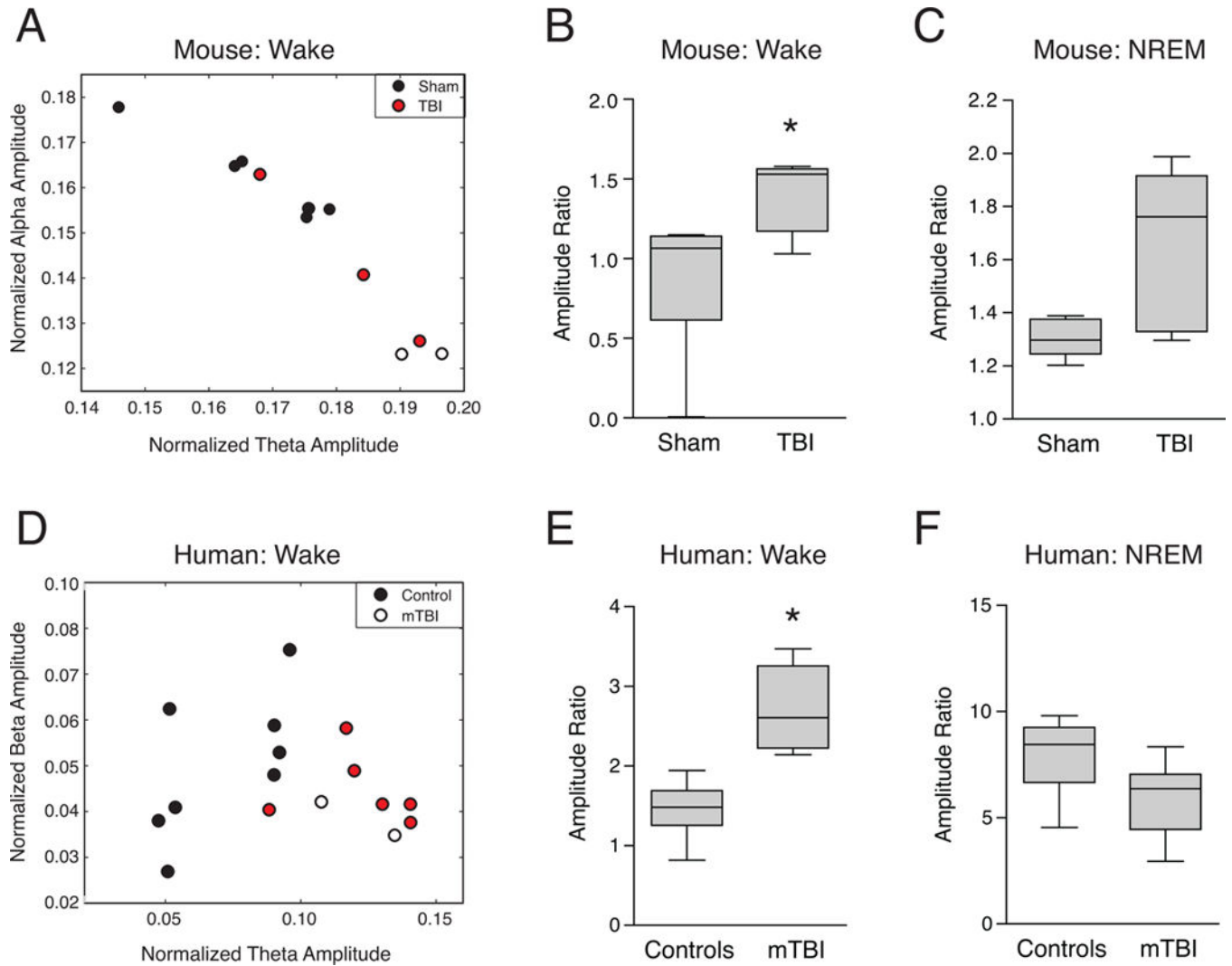


Figure 3. EEG amplitude ratios during the awake state significantly differ between TBI and sham injured mice, and also between human subjects with mTBI and controls

(A) Averaged theta:alpha amplitude ratios in mice with TBI (open circles) compared to sham control mice (black circles).

(B) Mice with TBI show significantly higher theta:alpha amplitude ratios during the awake state, but not during (C) NREM sleep, compared to sham-injured mice.

* $p < 0.01$ (Student's t-test, Bonferroni-adjusted for multiple comparisons)

(D) Averaged theta:beta amplitude ratios in human subjects with mTBI (open circles) compared to age-matched healthy control subjects (black circles).

(E) Human subjects with mTBI show significantly higher theta:beta amplitude ratios during the awake state, but not during (F) NREM sleep, compared to control subjects.

* $p < 0.01$ (Student's t-test, Bonferroni-adjusted for multiple comparisons)

Data in (B), (C), (E) and (F) are represented as Tukey Box and Whiskers plots, where the line within the gray boxes represents the median value, and the whiskers represent the 25th and 75th percentile values plus 1.5 times the interquartile difference.

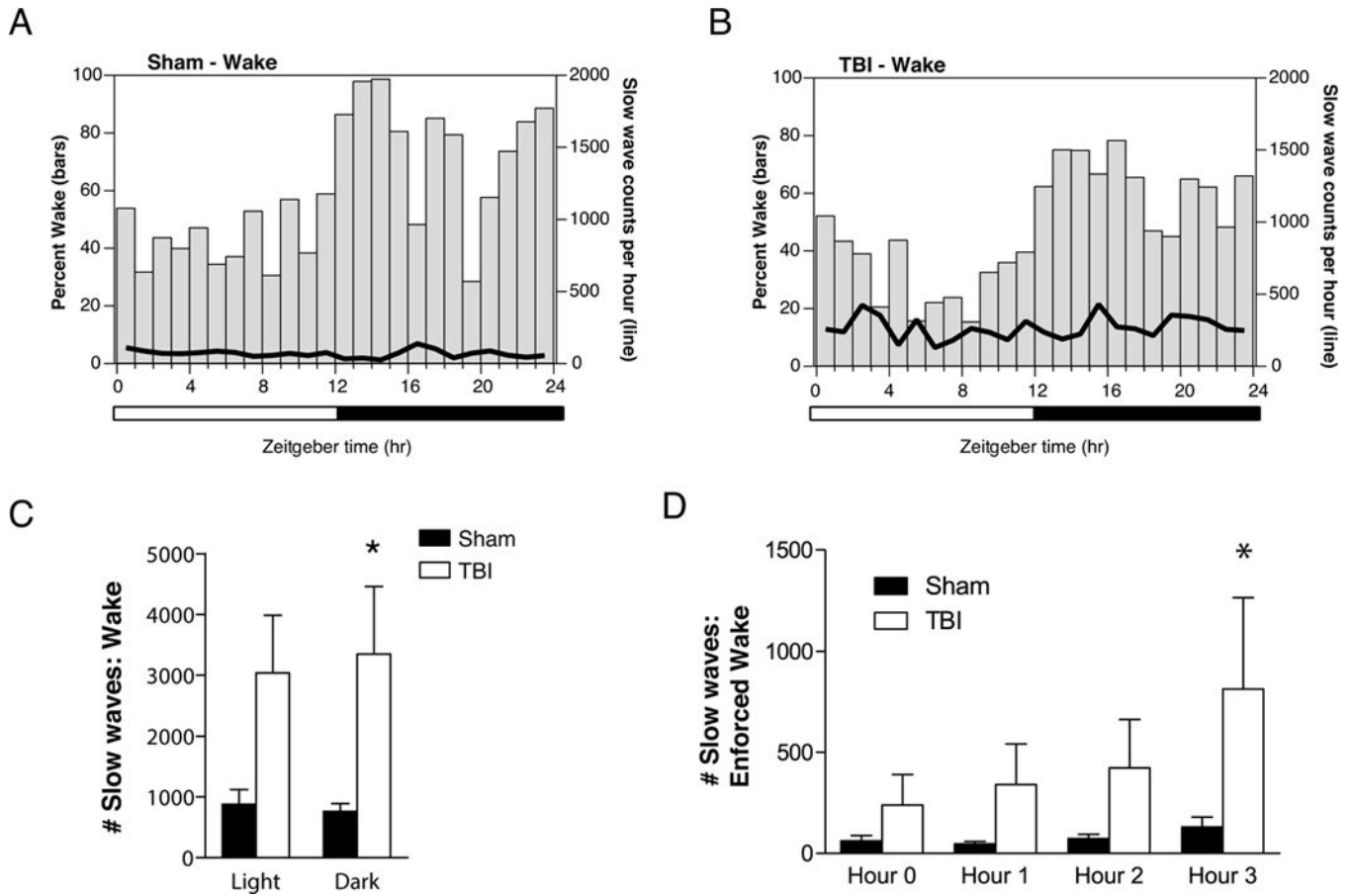


Figure 4. EEG slow wave counts in awake mice fluctuate over the 24-hour light:dark cycle, and increase during a period of enforced wakefulness

(A) Average number of EEG slow wave counts per hour during wake, superimposed upon percentage time spent awake per hour, over the 24-hour sleep-wake cycle in sham control mice.

(B) Average number of EEG slow wave counts per hour while awake, superimposed upon percentage time spent awake per hour, over the 24-hour sleep-wake cycle in mice with TBI.

(C) Comparison of the total slow wave counts over the 24-hour light:dark cycle across during the awake state for sham and TBI mice shows significantly higher slow wave counts during the dark phase in mice with TBI.

* $p < 0.05$, Two-way ANOVA, Bonferroni post-hoc test for significant main effect of Phase.

(D) Mice were kept awake for a short 3-hour period from ZT3-6 (10:00 am to 13:00 pm), a period notable for heightened sleep pressure. EEG slow wave counts from Hour 0 included only the spontaneously-occurring wake epochs from 9:00 to 10:00 am, and were corrected for the percentage of wake during each 30-min interval. EEG slow waves significantly increased with by Hour 3 of enforced waking in mice with TBI compared to sham control mice.

* $p < 0.05$, Two-way ANOVA, Bonferroni post-hoc test for significant main effect of Hour, and significant interaction between Hour and Injury.

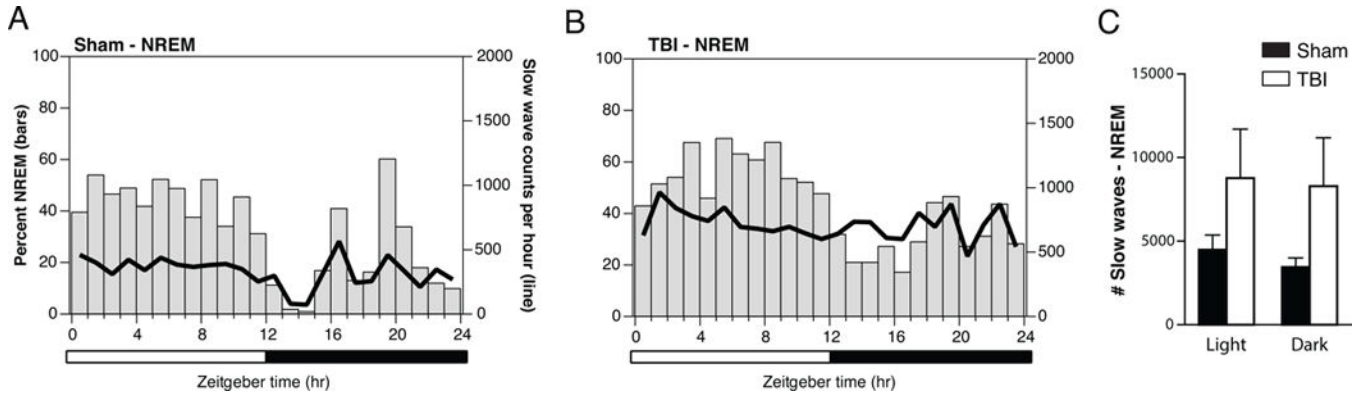


Figure 5. EEG slow wave counts during NREM sleep fluctuate over the 24-hour light:dark cycle, but do not significantly differ between TBI and sham-injured mice

(A) Average number of EEG slow waves counts per hour during NREM sleep, superimposed upon percentage time spent during NREM sleep per hour, over the 24-hour sleep-wake cycle in sham control mice.

(B) Average number of EEG slow waves counts per hour during NREM sleep, superimposed upon percentage time spent during NREM sleep per hour, over the 24-hour sleep-wake cycle in mice with TBI.

(C) Comparison of the total slow wave counts over the 24-hour light:dark cycle during NREM sleep between sham and TBI mice shows no significant group differences.

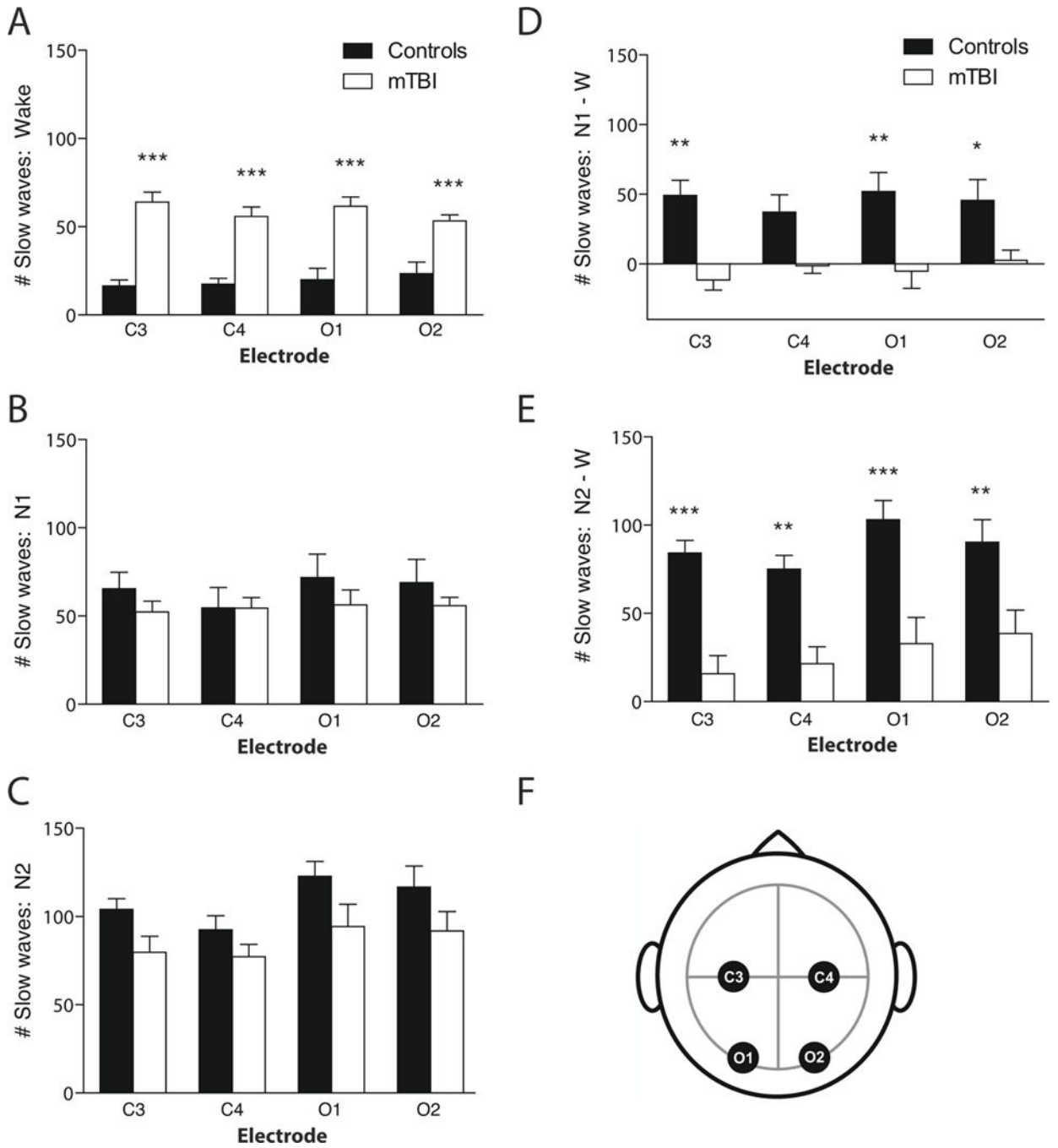


Figure 6. EEG slow wave counts while awake, but not during NREM sleep, are significantly greater across all channels in human subjects with mTBI

(A) Average number of EEG slow wave counts during the first wake epochs of the overnight polysomnography are significantly increased across C3, C4, O1 and O2 channels in human subjects with mTBI, compared to age-matched healthy control subjects.

*** $p < 0.001$, Two-way ANOVA, Bonferroni post-hoc test for significant main effect of Injury.

(B) Average number of EEG slow wave counts during NREM stage N1 sleep during the overnight polysomnography did not significantly differ between in human subjects with mTBI compared to age-matched healthy control subjects, in any channel.

(C) Average number of EEG slow wave counts during NREM stage N2 sleep during the overnight polysomnography did not significantly differ between in human subjects with mTBI compared to age-matched healthy control subjects, in any channel.

(D) Control subjects showed the expected increase in EEG slow waves in NREM stage N1 sleep compared to wake, whereas this increase was completely absent in mTBI subjects. * $p < 0.05$, ** $p < 0.01$, Two-way ANOVA, Bonferroni post-hoc test for significant main effect of Injury.

(E) Control subjects showed the expected increase in EEG slow waves in NREM stage N2 sleep compared to wake, whereas this increase was significantly smaller in mTBI subjects. ** $p < 0.01$, *** $p < 0.001$, Two-way ANOVA, Bonferroni post-hoc test for significant main effect of Injury.

(F) Schematic of EEG electrode lead placement on the human scalp. C3 = left central, C4 = right central, O1 = left occipital, O2 = right occipital.

Note that NREM stage N3 and REM were not analyzed due to the fact that not all subjects displayed these stages during polysomnography testing.

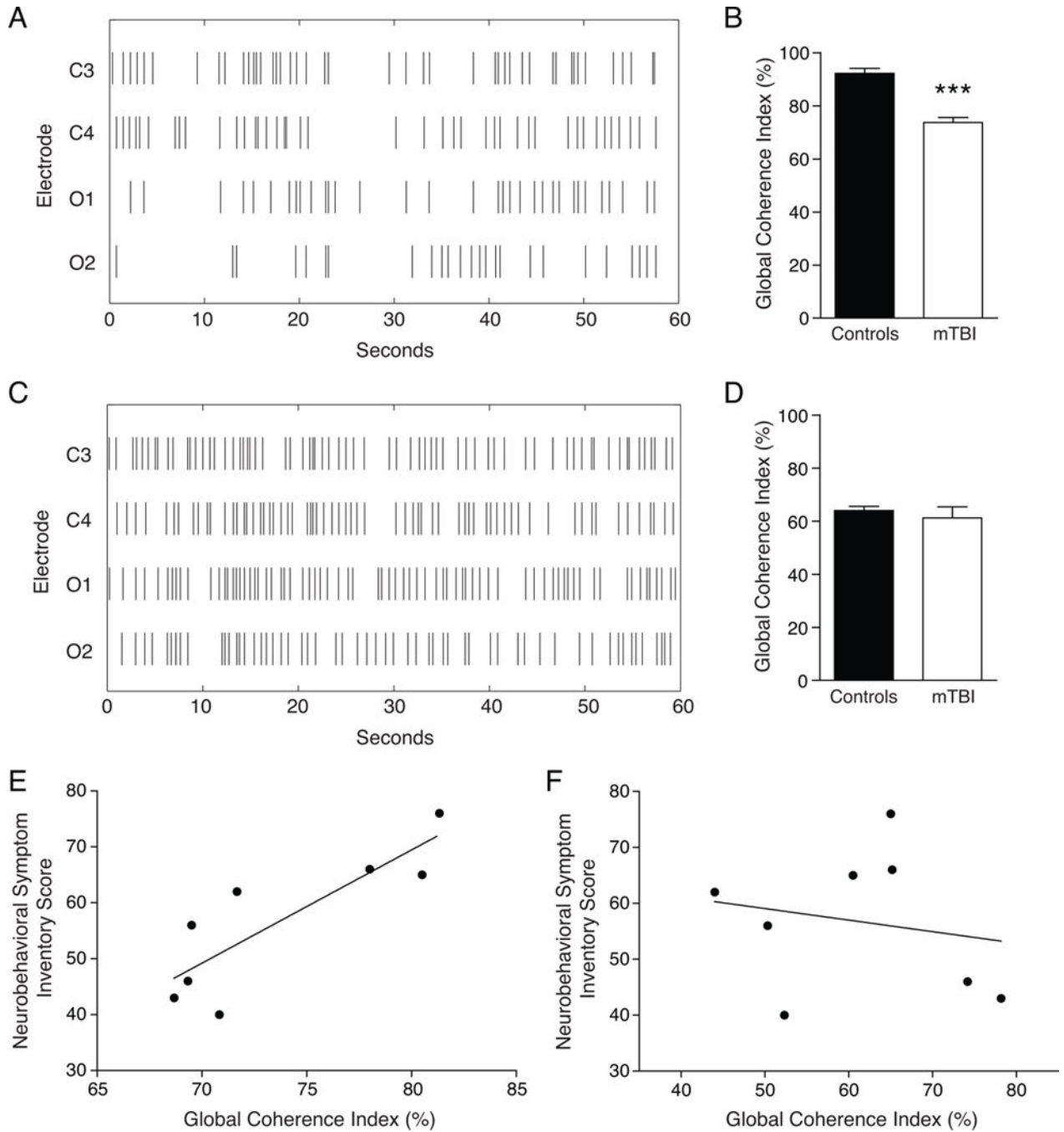


Figure 7. Global Coherence Index of EEG slow waves across channels in mTBI

(A) Raster plot showing temporal resolution of EEG slow waves across four channels during 60 seconds of wakefulness in a representative human subject with mTBI, compared to (C) NREM stage N2 sleep. The Global Coherence Index reflects the total percentage of 0.1 second bins containing consistent slow wave information across channels.

(B) Subjects with mTBI showed significantly lower coherence indices compared to controls. *** $p < 0.001$, Student's t-test. There was no difference between groups during NREM stage N2 sleep (D).

(E) The Global Coherence Index during wakefulness is significantly correlated with Neurobehavioral Symptom Inventory (NSI) score in human subjects with mTBI. $*p < 0.01$, Pearson's correlation, $R^2 = 0.71$. There was no significant correlation during NREM stage N2 sleep (F).

Table 1

Polysomnography characteristics in age-matched human subjects with mTBI and healthy control subjects.

	Controls		mTBI	
Age (years)	+/-	32.9	32.5	+/-
TST (min)	+/-	396.1	400.4	+/-
Sleep latency (min)	+/-	19.1	7.5	+/-
Sleep efficiency (%)	+/-	88.1	90.8	+/-
WASO (min)	+/-	33.7	22.1	+/-
N2 (%)	+/-	52.0	52.7	+/-
N3 (%)	+/-	13.7	16.1	+/-
REM (%)	+/-	19.6	12.2	+/-
AHI (events/hr)	+/-	1.8	7.2	+/-

Human subjects did not significantly differ in the following parameters: age, total sleep time, sleep efficiency, wake after sleep onset (WASO), or percentages of NREM stage N2 or N3 sleep. Subjects in the mTBI group showed shorter sleep latency, lower percentages of REM sleep, and mildly elevated AHI compared to controls.

Numbers listed as mean (SEM).

* $p < 0.05$,

** $p < 0.01$, Student's t-tests.

TST = total sleep time, WASO = wake after sleep onset, N2 = NREM stage N2 sleep, N3 = NREM stage N3 sleep, REM = rapid eye movement sleep, AHI = apnea-hypopnea index, SEM = standard error of the mean.